High-quality Wind Power Scenario Forecasts for Decision-making Under Uncertainty in Power Systems

Delikaraoglou, Stefanos; Pinson, Pierre

Published in:
Proceedings of 13th International Workshop on Large-Scale Integration of Wind Power and Transmission Networks

Publication date:
2014

Document Version
Peer reviewed version

High-quality Wind Power Scenario Forecasts for Decision-making Under Uncertainty in Power Systems

Stefanos Delikaraoglou and Pierre Pinson
Dept. of Electrical Engineering
Technical University of Denmark
Kgs. Lyngby 2800
stde@elektro.dtu.dk ppin@elektro.dtu.dk

***Abstract*—The large scale integration of wind generation in existing power systems requires novel operational strategies and market clearing mechanisms to account for the variable nature of this energy source. An efficient method to cope with this uncertainty is stochastic optimization which however requires high-quality forecasts in the form of scenarios. The main goal of this work is to release a public dataset of wind power forecasts to be used as a reference for future research. To that extent, we provide a complete framework to describe wind power uncertainty in terms of single-valued and probabilistic predictions as well as scenarios representing the spatio-temporal dependence structure of forecast errors. The applicability of the proposed framework is demonstrated with a small-scale stochastic unit commitment model.**

I. Introduction

The economic and environmental benefits from the growth of wind power have been important in recent years. However, wind power generation is highly variable and only partly predictable. This uncertainty poses new challenges both to system operators and wind power producers, considering that the balancing of forecast errors in real-time requires the activation of expensive reserves that increase systems costs and induce financial losses to the market players. Hence, the efficient wind power integration requires novel decision-making processes for the operation of the power system and re-design of the current market structure in order to account for the stochastic nature of this generation technology.

The existing setup of the European electricity markets involves two trading floors, the forward (day-ahead) and the real-time (balancing) market, which are cleared sequentially. The day-ahead market is settled 12 to 36 hours before actual power delivery, based on deterministic predictions for the uncertain parameters of the power system, e.g., wind generation. When the uncertainty reveals and the deviations from the day-ahead schedule are known, the real-time market is cleared in order to maintain the system balance.

This market architecture serves the requirements of a power system based on conventional generation where dispatch decisions need to be planned ahead and the balancing operation is driven by discrete disturbances that cannot be predicted in advance, e.g., outages of generators or transmission lines. However, the efficiency of this market design is disputed as the shares of intermittent renewables increase.

In order to account for the flexibility needs of the power system and take advantage of the - even partial - predictability of wind power, stochastic optimization models are gaining increased attention. In this context, [1] and [2] propose a joint clearing of the day-ahead and balancing markets cast as a two-stage stochastic programming problem. In a similar vein, [3] and [4] formulate a stochastic unit commitment model for the co-optimization of generation schedules and reserve requirements, while [5] proposes stochastic operational strategies for reserve activation. Nevertheless, stochastic programming presents a significant challenge regarding the uncertainty modeling in terms of scenarios, since their quality affects considerably the outcome of these models.

Most of the existing wind power prediction tools produce deterministic forecasts [6], which provide only a single value about the expected wind power. Recent research has also focused on probabilistic predictions [7], [8], giving the overall probability distribution of the power output and enabling the estimation of the marginal uncertainty, i.e., the probability distribution of prediction errors. However, probabilistic forecasts are still unable to model the development of these errors in space and in time. To capture this information, it is necessary to generate scenarios that respect both the spatial [9] and the temporal [10] interdependence structure of the forecast errors. These scenarios are suitable to be used in a stochastic optimization framework as previously discussed.

The purpose of this paper is to provide a methodological framework that describes the stochastic processes pertaining to wind power at different locations and forecast lead times. Wind power uncertainty is characterized in the form of point forecasts, probabilistic predictions as well as spatio-temporal scenarios of short-term wind power production. The main objective of this work is to release a dataset that can be used as a reference for studies that require advanced forecasting products; similarly to the IEEE test systems which are widely used by power system engineers as a basis for demonstrating the interest of their ideas.

The rest of the paper is organized as follows: Section II describes the forecasting methodologies to produce point and probabilistic predictions as well as spatio-temporal wind power scenarios. In Section III, these methods are applied to a case study using real wind power data and the applicability of this framework is illustrated in a small-scale stochastic unit commitment model. Finally, Section IV provides some relevant conclusions and suggestions for further work.

II. Wind power modeling and forecasting methodologies

This section provides an outline of the methodology used to generate different types of wind power forecasts. Single valued predictions (point forecasts) are produced using a Support Vector Regression (SVR) approach. Based on these point predictions, nonparametric probabilistic predictions are issued and their marginal distributions are retrieved. Finally, spatio-temporal wind power scenarios are obtained using Monte-Carlo sampling techniques.

A. Support vector regression for short-term power predictions

A powerful technique for forecasting applications is support vector regression (SVR), which is based on kernel regression and belongs to the family of machine learning methods. In case of wind power forecasting, the goal of the SVR algorithm is to find a direct mapping of wind speed on produced wind power. Let $p_{s,t}$ the actual wind power production at time t and location s, and $\hat{p}_{s,t+k|t}$, $\hat{u}_{s,t+k|t}$ the wind power and the speed forecasts respectively, issued at time t with leading horizon $h_k = 1, ...k, ..., d_k$. The SVR model aims to find a prediction function $\hat{g} : \mathbb{R}^u \times \mathbb{R}^h \times \mathbb{R}^p \to \mathbb{R}$ such that $\hat{p}_{t+k|t} = \hat{g}(\hat{u}_{s,t+k|t}, h_k, p_{s,t})$.

For a given set of training data $(\theta_1, \nu_1), \ldots, (\theta_i, \nu_i), \ldots, (\theta_n, \nu_n)$, where $\theta_i \in \Theta$ are the input patterns and ν_i the corresponding output values, the SVR algorithm finds a function $g(\theta)$ whose deviation from the actually obtained targets ν_i is less or equal to a predetermined non-negative value ε. This function should be able to balance the complexity and the amount of training errors according to the principle of Structural Risk Minimization [11].

Assuming that $g(\theta)$ is a linear function of the form $g(\theta) = \langle w, \theta \rangle + b$, $w \in \Theta, b \in \mathbb{R}$, the mathematical formulation of the optimization problem that SVR solves is

$$\min_{w,b,\xi,\xi^*} \quad \frac{1}{2}\|w\|^2 + C\sum_{i=1}^{n}(\xi_i + \xi_i^*) \tag{1}$$

s.t.

$$\nu_i - \langle w, \theta_i \rangle - b \leq \varepsilon + \xi_i \tag{2}$$

$$\langle w, \theta_i \rangle + b - \nu_i \leq \varepsilon + \xi_i^* \tag{3}$$

$$\xi, \xi^* \geq 0 \tag{4}$$

where $\|w\|$ is the Euclidean norm defining the flatness of the regression function and $\langle \cdot, \cdot \rangle$ the dot product in Θ. It holds that $\|w\|^2 = \langle w, w \rangle$. The slack variables ξ_i and ξ_i^* are used in order to relax the constraints related to the ε-insensitive region, such as only the points that are located outside this region are penalized [12].

The objective function (1) consists of two terms. The first term, $\frac{1}{2}\|w\|^2$, represents the degree of complexity, i.e., the flatness of the function. The second term, $\sum_{i=1}^{n}(\xi_i + \xi_i^*)$, corresponds to the tolerance for deviations larger than ε. The manually adjustable constant C determines the trade-off between these two properties of the function.

In cases where the dimensionality of w is much higher than the number of observations as well as in order to extend the SVR algorithm to non-linear functions, it is useful to solve the dual formulation of the problem (1)-(4) [12]. This dual problem is written as

$$\max_{\lambda,\lambda^*} -\frac{1}{2}\sum_{i,j=1}^{n}(\lambda_i - \lambda_i^*)(\lambda_j - \lambda_j^*)\langle \theta_i, \theta_j \rangle - \varepsilon\sum_{i=1}^{n}(\lambda_i + \lambda_i^*) + \sum_{i=1}^{n}\nu_i(\lambda_i - \lambda_i^*) \tag{5}$$

s.t.

$$\sum_{i=1}^{n}(\lambda_i - \lambda_i^*) = 0 \tag{6}$$

$$\lambda_i, \lambda_i^* \in [0, C] \tag{7}$$

The optimization variables of the dual problem are the Lagrange multipliers λ_i, λ_i^* that correspond to constraints (2) and (3) of the primal problem (1)-(4). If a point θ_i lies within the ε-insensitive region the corresponding λ_i and λ_i^* are equal to zero. The SVR regression function can be formulated as

$$g(\theta) = \sum_{i=1}^{n}(\lambda_i - \lambda_i^*)\langle \theta_i, \theta \rangle + b \tag{8}$$

where $\boldsymbol{\theta}$ is the vector of the independent variables for the new input points. It should be noted that the above formulation does not require the explicit calculation of w but only the dot products between the data.

In order to obtain a nonlinear regression function, the training data θ_i can be transformed using a map $\Psi : \Theta \to \mathcal{F}$. Then, a linear regression function can be constructed in this new feature space $\mathcal{F}$ according to the procedure described above. Given the property of the SVR algorithm that requires only the calculation of the dot products between the data, a kernel function $K(\theta, \theta')$ can be used in order to write the dot product as $\langle \Psi(\theta), \Psi(\theta') \rangle = K(\theta, \theta')$. This implies that there is no need to know the explicit form of any vector in the transformed space, since the dot products can be directly calculated by the chosen kernel. The optimization problem that the SVR solves in the non-linear case is identical to (5)-(7), where the the vectors θ_i are replaced with the transformed vectors $\Psi(\theta_i)$. The manually adjustable parameters that control the regression quality are the cost of error C, the width ε and the kernel function K.

B. Probabilistic forecasts using nonparametric probabilistic distributions

Probabilistic forecasts are considered in form of nonparametric predictive densities, where the cumulative distribution functions of wind power production are described by a set of quantile forecasts. Being at time t and for location s, write $\hat{f}_{s,t+k|t}$ the probabilistic forecast of the density function of wind power production $p_{s,t+k}$ at time $t + k$ and $\hat{F}_{s,t+k|t}$ the corresponding cumulative distribution function. Given that $\hat{F}_{s,t+k|t}$ is a strictly increasing function, every quantile $\hat{q}_{s,t+k|t}^{(\alpha_i)}$ with nominal proportion α_i, i.e., the predicted power value which has probability α_i to cover the observation, is uniquely defined as

$$\hat{q}_{s,t+k|t}^{(\alpha_i)} = \hat{F}_{s,t+k|t}^{-1}(\alpha_i). \tag{9}$$

Consequently, a nonparametric forecast $\hat{F}_{s,t+k|t}$ can be assembled as

$$\hat{F}_{s,t+k|t} = \left\{ \hat{q}^{(\alpha_i)}_{s,t+k|t} | 0 \leq \alpha_1 < ... < \alpha_i < ... \leq 1 \right\}. \quad (10)$$

In practical applications a continuous $\hat{F}_{s,t+k|t}$ function is approximated by a smooth curve over the available quantile forecasts, while the tails of the predictive distribution can be modeled with exponential tails to reflect properly the full range of possible outcomes [13].

The quantile regression model employed in this work is based on the methodology described in [14]. For a training set of data $(\hat{p}_{s,t+k|t}, p_{s,t+k})$, each quantile $\hat{q}^{(\alpha_i)}$ is calculated by a parametric function $\eta(\hat{p}_{s,t+k|t}, \boldsymbol{\beta}^{(\alpha_i)})$, where $\boldsymbol{\beta}^{(\alpha_i)}$ is a vector of model parameters, estimated by solving the following optimization problem

$$\hat{\boldsymbol{\beta}}^{(\alpha_i)} = \arg\min_{\boldsymbol{\beta}} \sum_{i=1}^{n} \rho_{\alpha_i}(p_{s,t+k} - \eta(\hat{p}_{s,t+k|t}, \boldsymbol{\beta}^{(\alpha_i)})). \quad (11)$$

In the above formulation ρ_{α_i} is the tilted absolute function defined as

$$\rho_{\alpha_i}(u) = u(\alpha_i - \mathbb{1}(u < 0)). \quad (12)$$

C. Spatio-temporal scenarios of wind power generation

Aiming to produce wind power scenarios that respect the spatio-temporal interdependence structure of the forecast errors, we employ an extended version of the method presented in [10] and [9] which focus solely on the temporal and spatial dependencies, respectively.

Denoting by d_s and d_k the number of locations and lead times respectively, the overall dimension of the scenario generation problem is $d = d_s \times d_k$. Assuming that the spatio-temporal dependence structure can be modeled by a Gaussian copula, the covariance matrix $\boldsymbol{\Sigma} \in \mathbb{R}^{d \times d}$ of a d-dimensional standard normal random variable $\mathbf{X}_t \sim \mathcal{N}_d(0, \boldsymbol{\Sigma})$ fully captures the interdependence structure, for all lead times and locations. Given the assumption of the Gaussian meta-model, the diagonal elements of $\boldsymbol{\Sigma}$ are equal to 1, while the off-diagonal elements represent the correlation between the corresponding random variables.

Write $Y_{s,k}$ the random variable whose realization at time t is defined as

$$Y^{(t)}_{s,k} = \hat{F}_{s,t+k|t}(p_{s,t+k}), \quad \forall t, \forall s, \forall k \quad (13)$$

and follows a uniform distribution, $Y_{s,k} \sim \mathcal{U}[0,1]$. Then, a standard normal random variable $X_{s,k} \sim \mathcal{N}(0,1)$ is obtained using the following transformation

$$X^{(t)}_{s,k} = \Phi^{-1}\left(Y^{(t)}_{s,k}\right), \quad \forall t, \forall s, \forall k \quad (14)$$

where Φ^{-1} is the inverse of the Gaussian cumulative distribution function. Applying this transformation into all uniform variables $Y^{(t)}_{s,k}$, for all the locations and lead times, one obtains d standard Gaussian variables, whose multivariate structure is described by $\boldsymbol{\Sigma}$. The covariance matrix $\boldsymbol{\Sigma}$ is estimated based on historical data (i.e., a training period with $t = 1, \ldots, \tilde{T}$) using the following expression

$$\boldsymbol{\Sigma} = \sum_{t=1}^{\tilde{T}} \mathbf{X}_t \mathbf{X}_t^{\top} \quad (15)$$

where

$$\mathbf{X}_t = \begin{pmatrix} \Phi^{-1}\left(\hat{F}_{s_1,t+1|t}(p_{s_1,t+1})\right) \\ \cdots \\ \Phi^{-1}\left(\hat{F}_{s_1,t+d_k|t}(p_{s_1,t+d_k})\right) \\ \vdots \\ \Phi^{-1}\left(\hat{F}_{s_{d_s},t+1|t}(p_{s_{d_s},t+1})\right) \\ \cdots \\ \Phi^{-1}\left(\hat{F}_{s_{d_s},t+d_k|t}(p_{s_{d_s},t+d_k})\right) \end{pmatrix} \quad (16)$$

is the vector of previous measurements transformed through the probabilistic forecast series issued at time t and the probit function Φ^{-1}. In practical applications the covariance matrix can be adaptively estimated using a recursive estimation method as discussed in [10]. In order to ensure that $\boldsymbol{\Sigma}$ is a suitable covariance matrix of a unit multivariate Normal variable, the following transformation is applied

$$\boldsymbol{\Sigma} = \boldsymbol{\Sigma} \oslash (\boldsymbol{\sigma}_t \boldsymbol{\sigma}_t^{\top}) \quad (17)$$

where $\boldsymbol{\sigma}_t$ is the vector of standard deviations and $\oslash$ denotes the element-by-element division.

For the generation of a set of Ω spatio-temporal scenarios, a multivariate Normal random number generator with zero mean and covariance matrix $\boldsymbol{\Sigma}$ is used to draw Ω realizations of $\mathbf{X}_t$. Then, for every lead time and every location, the inverse probit function Φ is applied to each element $X^{(\omega)}_{s,k}$ of $\mathbf{X}_t$ in order to obtain Ω realizations of $Y^{(\omega)}_{s,k}$ as

$$Y^{(\omega)}_{s,k} = \Phi(X^{(\omega)}_{s,k}) \ \ \forall s, \forall k, \forall \omega \quad (18)$$

Finally, the trajectories of wind power generation that respect the predictive densities of the probabilistic forecasts are obtained using the following transformation

$$\hat{p}^{(\omega)}_{s,t+k|t} = \hat{F}^{-1}_{s,t+k|t}(Y^{(\omega)}_{s,k}) \ \ \forall s, \forall k, \forall \omega. \quad (19)$$

III. Case Study

A. Wind Data

The methodologies described in Section II for issuing different types of wind power forecasts are applied using a dataset of wind speed predictions from the European Centre for Medium-range Weather Forecasts [15] combined with publicly available wind power measurements provided by the Australian Energy Market Operator [16]. Both datasets contain information for the years 2012 and 2013. The wind speed predictions are issued at 00:00 and 12:00 of each day and they have an hourly resolution up to 72-hour ahead. The wind power dataset contains measurements, with 5-minute resolution, for 22 wind farms located in Western Australia. For the purpose of this study, hourly wind generation is obtained as the average production over the corresponding 5-minute intervals. All measurements are normalized by the nominal capacity of the wind farm and hence they take values in the unit interval.

B. Application and results of the forecasting methodologies

In the present study, the data for year 2012 are used to train the forecast models which are then applied on the data from 2013 to produce a complete dataset of forecasts. For the

generation of point forecasts, the SVR method employing the RBF kernel function is implemented using the open-access package LIBSVM [17]. The range of the optimal parameters for the SVR model follows the suggestions of [18] for similar wind power forecasting applications and the parameter selection is performed using k-fold cross validation. Finally, the parameters are selected according to the minimum mean squared error (MSE) criterion [19]. For the nonparametric forecasts, predictive distributions are given by 19 quantile forecasts with nominal proportions from 0.05 to 0.95 by 0.05 increments. The quantile regression model uses as explanatory variables the single value predictions obtained from the SVR model. All the computational models for the quantile regression and scenario generation are developed in open-source Python scripts which are publicly available along with the final forecasting dataset at [20].

Figure 1 depicts an example of probabilistic predictions along with the corresponding point forecasts and the actual measurements. Figure 2 presents an example of space-time scenarios of short-term wind power production for the same episode as Fig. 1. The average of a high number of scenarios generated with the proposed method would be equivalent to the point predictions of Fig. 1, since they are the mean of all possible outcomes. The quality of the generated wind power forecasts is at the state-of-the-art level, as verified with a number of error criteria, e.g., Mean Absolute Error (MAE) and Root Mean Square Error (RMSE).

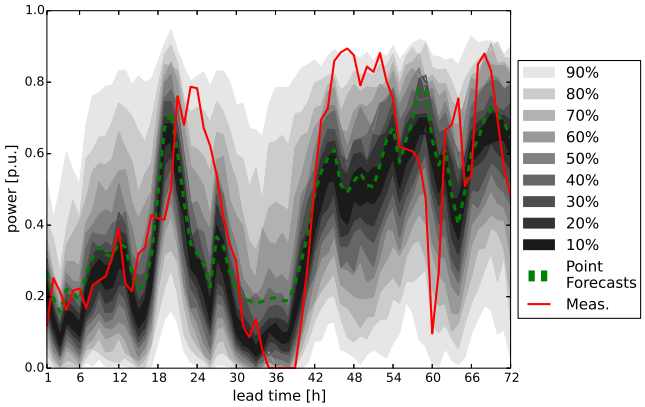

Fig. 1: Nonparametric probabilistic forecasts of wind power production with nominal coverage rates of the prediction intervals 10, 20,..., and 90%, produced with quantile regression, accompanied with the corresponding point forecasts and measurements.

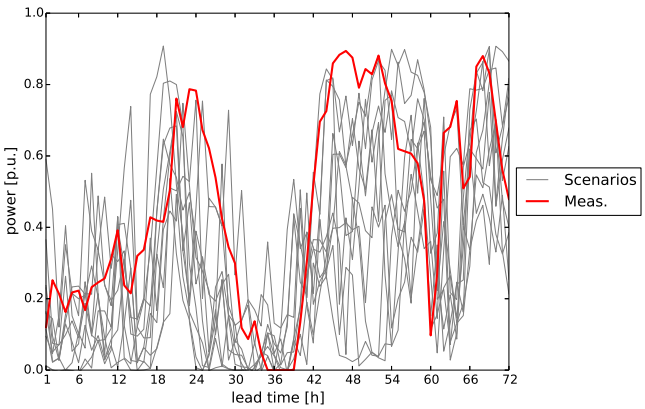

Fig. 2: Example of 10 spatio-temporal scenarios of wind power production (for the same period and location as in Fig. 1).

C. Stochastic unit commitment model

In order to demonstrate the use of the wind power forecasts on power system and electricity market studies, we consider the following two-stage stochastic unit commitment model, where the first stage represents the day-ahead schedule and the second stage represents the real-time dispatch, i.e, the decisions which can be modified once the uncertainty is revealed. This optimization model is a mixed integer linear programming problem (MILP) due to the binary variables modeling the on/off status of the generators.

$$\min_{\Xi} \sum_t \sum_i C_i P_{i,t} + \sum_t \sum_i C_i^{SU} y_{i,t} + \sum_t \sum_i C_i^{SD} z_{i,t} + \sum_t \sum_\omega \pi_\omega \left[\sum_i (C_i^U r_{i,\omega,t}^U - C_i^D r_{i,\omega,t}^D) + \sum_n V^{LOL} L_{n,\omega,t}^{shed} + \sum_n V^{WSP} W_{n,\omega,t}^{spill} \right] \quad (20)$$

s.t.

Generation constraints:

$$u_{i,t} \geq \sum_{\tau=t-UT_i+1}^{t} y_{i,\tau}, \quad \forall\, i, \forall t \quad (21)$$

$$1 - u_{i,t} \geq \sum_{\tau=t-DT_i+1}^{t} z_{i,\tau}, \quad \forall\, i, \forall t \quad (22)$$

$$y_{i,t} - z_{i,t} = u_{i,t} - u_{i,t-1}, \quad \forall\, i, \forall t \quad (23)$$

$$y_{i,t} + z_{i,t} \leq 1, \quad \forall\, i, \forall t \quad (24)$$

$$u_{i,t} \geq y_{i,t}, \quad \forall\, i, \forall t \quad (25)$$

$$u_{i,t} \geq z_{i,t+1}, \quad \forall\, i, \forall t \quad (26)$$

$$P_{i,t} + r_{i,\omega,t}^U \leq P_{i,t-1} + r_{i,\omega,t-1}^U + RU_i(u_{i,t-1} + y_{i,t}), \quad \forall\, i, \forall t, \forall \omega \quad (27)$$

$$P_{i,t-1} - r_{i,\omega,t-1}^D \leq P_{i,t} - r_{i,\omega,t}^D + RD_i(u_{i,t} + z_{i,t}), \quad \forall\, i, \forall t, \forall \omega \quad (28)$$

$$P_{i,t} + r_{i,\omega,t}^U \leq P_i^{\max} \cdot (u_{i,t} - z_{i,t+1}) + RD_i \cdot z_{i,t+1}, \quad \forall\, i, \forall t, \forall \omega \in \Omega \quad (29)$$

$$P_{i,t} - r_{i,\omega,t}^D \geq P_i^{\min} \cdot u_{i,t}, \quad \forall\, i, \forall t, \forall \omega \quad (30)$$

$$r_{i,\omega,t}^U \leq R_i^{U,max}, \quad \forall i, \forall t, \forall \omega \quad (31)$$

$$r_{i,\omega,t}^D \leq R_i^{D,max}, \quad \forall i, \forall t, \forall \omega \quad (32)$$

$$W_{n,t}^s \leq W_n^{max}, \quad \forall n, \forall t \quad (33)$$

$$W_{n,\omega,t}^{spill} \leq W_{n,\omega,t}, \quad \forall n, \forall t, \omega \quad (34)$$

Power system constraints- Day-ahead stage:

$$\sum_i A_{n,i}^{n2i} \cdot P_{i,t} + W_{n,t}^s = \sum_d A_{n,j}^{n2j} \cdot L_{j,t} + \sum_l A_{n,l}^{n2l} \cdot fl_{l,t}^{DA}, \quad \forall t, \forall n \quad (35)$$

$$fl_{l,t}^{DA} = \sum_n B_{l,n} \cdot \delta_{n,t}^{DA}, \quad \forall t, \forall l \quad (36)$$

$$-fl_l^{max} \leq fl_{l,t}^{DA} \leq fl_l^{max}, \quad \forall t, \forall l \quad (37)$$

Power system constraints - Balancing stage:

$$\sum_i A^{n2i}_{n,i} \cdot \left(r^U_{i,\omega,t} - r^D_{i,\omega,t}\right) + L^{shed}_{n,\omega,t} + W_{n,\omega,t} - W^s_{n,t} - W^{spill}_{n,\omega,t} = \sum_l A^{n2l}_{n,l} \cdot \left(fl^{RT}_{l,\omega,t} - fl^{DA}_{l,t}\right), \forall t, \forall \omega, \forall n \quad (38)$$

$$fl^{RT}_{l,\omega,t} = \sum_n B_{l,n} \cdot \delta^{RT}_{n,\omega,t}, \quad \forall t, \forall l, \forall \omega \quad (39)$$

$$-fl^{max}_l \leq fl^{RT}_{l,\omega,t} \leq fl^{max}_l, \quad \forall t, \forall l, \forall \omega \quad (40)$$

$$l^{shed}_{n,\omega,t} \leq \sum_j A^{n2j}_{n,j} \cdot L_{j,t}, \quad \forall n, \forall t, \forall \omega \quad (41)$$

where $\Xi = \{P_{i,t}, u_{i,t}, y_{i,t}, z_{i,t}, W^s_{n,t}, \delta^{DA}_{n,t}, \delta^{RT}_{n,\omega,t}, r^U_{i,\omega,t}, r^D_{i,\omega,t}, L^{shed}_{n,\omega,t}, W^{spill}_{n,\omega,t}\}$ is the set of the optimization variables. The notation used here follows the one in [21]. Additional symbols are: i) indices l and t denote the lines and the time periods, ii) C^{SU} and C^{SD} denote the start-up and shut-down costs, iii) C^U and C^D denote the energy sale and purchase price in the balancing market, iv) UT and DT denote the minimum up and down time, v) RU and RD denote the ramping up and down rate, vi) binaries y, z and u are equal to 1 if the unit is starting up, shuting down and is online respectively, vii) fl denotes the power flow and viii) $A^{\dagger 2 \ddagger}$ denotes the mapping from set $\dagger$ into the set $\ddagger$.

The objective function (20) aims to minimize the expected cost of power system which is made up of the day-ahead and the balancing cost components. The day-ahead cost includes the energy production, the start-up and the shut-down costs. In real-time operation additional costs arise from the reserve deployment, the wind spillage and the load shedding.

The set of *Generation constraints* (21)-(34) model the technical limitations of the power generating units. In particular, constraints (21) and (22) enforce the minimum up and down time, while constraints (23) - (26) represent the commitment status of the conventional units. The set of constraints (27)- (28) and (29) - (30) specify the ramping and the power production limits respectively, for each generator. Finally, constraints (31) - (32) ensure that dispatched reserves are lower or equal to the reserve capacity limits of each unit and constraints (33) - (34) limit the dispatched wind production and the wind spillage to the wind farm capacity and the realized wind power production respectively. The set of *Power system constraints* includes the power balance equations for the day-ahead (35) and the real-time (38) operation. In addition, the power flow and the transmission capacity limits of each line are modeled through constraints (36) - (37) and (39) - (40) for the two stages respectively. Constraint (41) ensures that the amount of load shed is smaller than or equal to the actual load consumption.

The stochastic unit commitment model is applied to a modified IEEE 14-bus system [22] shown in Fig. 3, which includes four conventional generators and two wind farms. The technical and the economic data of the system are given in Tables I-V. The wind farms located at nodes 5 and 13 have installed capacity of 50 MW and 25 MW respectively and their power production is modeled using a set of spatio-temporal scenarios from the available dataset which present minimal correlation in generation and forecast errors. The value of lost load V^{LOL} is set to 200$/MWh while the cost of wind curtailment V^{WSP} is zero.

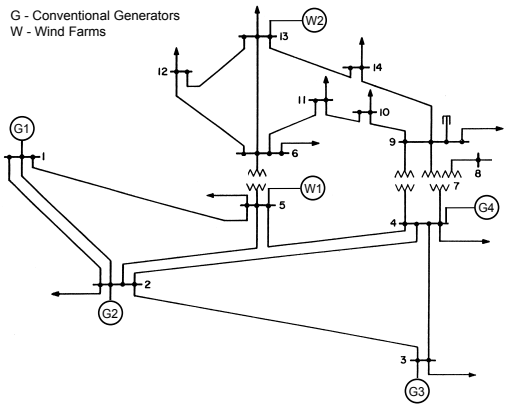

Fig. 3: Network topology 14-bus power system

TABLE I: Generator data

Unit	P^{max} [MW]	P^{min} [MW]	R^+ [MW]	R^- [MW]	RU [MW/h]	RD [MW/h]	UT [h]	DT [h]
G1	60	12	50	50	60	60	3	2
G2	130	26	40	40	130	130	8	4
G3	170	34	30	30	120	120	8	4
G4	190	38	30	30	120	120	8	8

Figure 4 presents the production schedule of the units for the 24 hours of the day. It can be observed that most of the system demand is covered by Units 3 and 4, which have the lowest production costs. Especially, Unit 4 is fully dispatched during the whole day, apart from the first period due to the ramping constraints. Units 2 and 3 serve mainly the intermediate load of the system whereas Unit 1 is dispatched only in periods 17-19 in order to cover the peak demand. In addition, up and down regulation is provided by Units 2 and 3 to cover any real-time imbalances. The amount of dispatched wind power varies during the day according to scenario forecasts, the technical constraints of the system and the network topology. Table VI shows the day-ahead and the expected balancing and total operating costs of the power system. It should be noted that the expected balancing cost is negative because of the down regulation needs arising from the wind uncertainty.

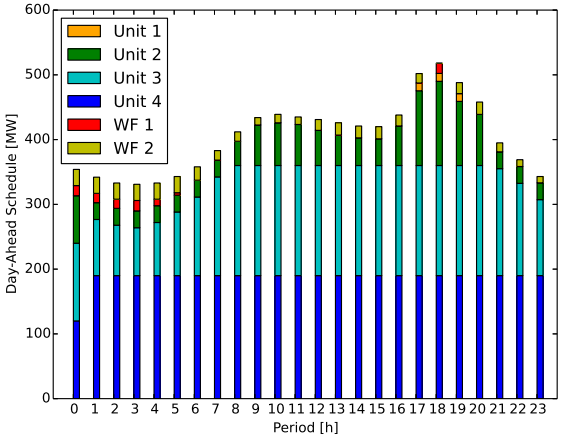

Fig. 4: Optimal generation schedule

TABLE II: Unit costs and initial state

Unit	C [$/MWh]	C^U [$/MWh]	C^D [$/MWh]	C^{SU} [$]	C^{SD} [$]	P_{ini} [MW]	U_{ini} [0/1]	T_{ini} [h]
G1	35	37	34	500	250	0	0	-20
G2	25	27	24	1000	500	0	0	-20
G3	20	22	19	1400	600	0	0	-20
G4	15	17	14	1500	700	0	0	-20

TABLE III: Load profile

Hour	System Demand [MW]	Hour	System Demand [MW]
1	355.754	13	430.768
2	340.531	14	426.022
3	332.853	15	421.638
4	330.656	16	419.929
5	332.915	17	437.141
6	341.226	18	500.839
7	358.334	19	518.600
8	383.929	20	488.424
9	411.442	21	458.467
10	433.856	22	394.881
11	439.213	23	367.183
12	435.628	24	341.675

IV. Conclusions and Future work

This paper presented a complete methodological framework for the generation of different types of wind power forecasts; namely point and probabilistic predictions as well as spatio-temporal scenarios. This framework was applied to real wind power measurements combined with state-of-the-art wind speed predictions in order to produce a publicly available dataset of high-quality forecasts. The applicability of these products was illustrated in a stochastic unit commitment model. Future work will focus on further improvement of the forecasting products and their application in larger scale decision-making problems.

Acknowledgment

The authors would like to thank Christos Ordoudis (Technical University of Denmark) for providing the setup of the stochastic unit commitment model and Jethro Dowell (University of Stathclyde) for his assistance in data handling. Stefanos Delikaraoglou is funded by Energinet.dk in support of ERA-Net SmartGrids through the project "BPES - Balancing power in the European system", No. 2010-1-10816. Pierre Pinson is partly supported by the Danish Council for Strategic Research (DSF) through the project "5s-Future Electricity Markets", No. 12-132636/DSF.

References

[1] J. M. Morales, A. J. Conejo, K. Liu, and J. Zhong, "Pricing electricity in pools with wind producers," *Power Systems, IEEE Transactions on*, vol. 27, no. 3, pp. 1366–1376, 2012.

[2] G. Pritchard, G. Zakeri, and A. Philpott, "A single-settlement, energy-only electric power market for unpredictable and intermittent participants," *Operations research*, vol. 58, no. 4 (2), pp. 1210–1219, 2010.

[3] A. Papavasiliou, S. S. Oren, and R. P. O'Neill, "Reserve requirements for wind power integration: A scenario-based stochastic programming framework," *Power Systems, IEEE Transactions on*, vol. 26, no. 4, pp. 2197–2206, 2011.

[4] A. Tuohy, P. Meibom, E. Denny, and M. O'Malley, "Unit commitment for systems with significant wind penetration," *Power Systems, IEEE Transactions on*, vol. 24, no. 2, pp. 592–601, 2009.

[5] S. Delikaraoglou, K. Heussen, and P. Pinson, "Operational strategies for predictive dispatch of control reserves in view of stochastic generation," in *Power Systems Computation Conference (PSCC), Wroclaw, Poland, Aug 18-22, 2014*. IEEE, 2014, pp. 1–7.

TABLE IV: Distribution of system load

Load	Node	% of system load	Load	Node	% of system load
Load 1	2	8.37	Load 7	10	3.47
Load 2	3	36.33	Load 8	11	1.35
Load 3	4	18.43	Load 9	12	2.35
Load 4	5	2.93	Load 10	13	5.32
Load 5	6	4.32	Load 11	14	5.75
Load 6	9	11.38			

TABLE V: Transmission line parameters

From	To	Reactance [p.u.]	Capacity [MVA]	From	To	Reactance [p.u.]	Capacity [MVA]
1	2	0.0592	480	6	11	0.1989	72
1	5	0.223	260	6	12	0.2558	128
2	3	0.198	144	6	13	0.1303	128
2	4	0.1763	260	7	8	0.1762	128
2	5	0.1739	200	7	9	0.11	128
3	4	0.171	260	9	10	0.0845	128
4	5	0.0421	180	9	14	0.2704	128
4	7	0.2091	220	10	11	0.1921	48
4	9	0.5562	128	12	13	0.1999	48
5	6	0.252	180	13	14	0.348	48

TABLE VI: System cost

	Expected Total	Expected Balancing	Day-ahead	Start-up	Shut-down
Cost ($)	171092.3	-1930.2	168372.5	4400	250

[6] G. Giebel, R. Brownsword, G. Kariniotakis, M. Denhard, and C. Draxl, "The state-of-the-art in short-term prediction of wind power: A literature overview," ANEMOS. plus, Tech. Rep., 2011.

[7] Y. Zhang, J. Wang, and X. Wang, "Review on probabilistic forecasting of wind power generation," *Renewable and Sustainable Energy Reviews*, vol. 32, pp. 255–270, 2014.

[8] P. Pinson, "Wind energy: Forecasting challenges for its operational management," *Statistical Science*, vol. 28, no. 4, pp. 564–585, 2013.

[9] G. Papaefthymiou and P. Pinson, "Modeling of spatial dependence in wind power forecast uncertainty," in *Probabilistic Methods Applied to Power Systems, 2008. PMAPS'08. Proceedings of the 10th International Conference on*. IEEE, 2008, pp. 1–9.

[10] P. Pinson, H. Madsen, H. A. Nielsen, G. Papaefthymiou, and B. Klöckl, "From probabilistic forecasts to statistical scenarios of short-term wind power production," *Wind energy*, vol. 12, no. 1, pp. 51–62, 2009.

[11] B. Schölkopf and A. J. Smola, *Learning with kernels: support vector machines, regularization, optimization, and beyond*. MIT press, 2002.

[12] A. J. Smola and B. Schölkopf, "A tutorial on support vector regression," *Statistics and computing*, vol. 14, no. 3, pp. 199–222, 2004.

[13] T. Jónsson, P. Pinson, H. Madsen, and H. A. Nielsen, "Predictive densities for day-ahead electricity prices using time-adaptive quantile regression," *European Journal of Operational Research*, 2014.

[14] R. Koenker, *Quantile regression*. Cambridge university press, 2005.

[15] ECMWF [Online]. Available:http://www.ecmwf.int.

[16] AEMO [Online]. Available: www.aemo.com.au.

[17] C.-C. Chang and C.-J. Lin, "LIBSVM: a library for support vector machines," *ACM Transactions on Intelligent Systems and Technology (TIST)*, vol. 2, no. 3, p. 27, 2011.

[18] O. Kramer and F. Gieseke, "Short-term wind energy forecasting using support vector regression," in *Soft Computing Models in Industrial and Environmental Applications, 6th International Conference SOCO 2011*. Springer, 2011, pp. 271–280.

[19] S. R. Gunn *et al.*, "Support vector machines for classification and regression," *ISIS technical report*, vol. 14, 1998.

[20] Wind power predictions dataset for Western Australia 2012-2013. [Online]. Available: http://pierrepinson.com/?page_id=992

[21] J. M. Morales, A. J. Conejo, and J. Pérez-Ruiz, "Economic valuation of reserves in power systems with high penetration of wind power," *Power Systems, IEEE Transactions on*, vol. 24, no. 2, pp. 900–910, 2009.

[22] University of Washington. Power system test case archive. [Online]. Available: http://www.ee.washington.edu/research/pstca/